

Interpretation on Breast Cancer Generation in 2D & 3D Images by Skeletonization Algorithm

Madhavi Pingili, E G Rajan

Abstract: The present usage and values obtained clinically on breast cancer expansion and assessment techniques are tragically not upto the mark. In this advanced world, 3D mammography algorithm is not used till now for identifying cancer expansion. A specialized algorithm called skeletonization algorithm is used after identifying the cancer in women's breast and estimating the direction of spreading cancer and its malignancy. For this 2D and 3D breast images are taken for clinical experiment.

Keywords: Breast Cancer, Lactal Carcinoma, 2D Breast Cancer Spread, 3D Breast Cancer Spread

I. INTRODUCTION

In this paper a 2D and 3D mammography breast images are taken for proposing a narrative procedure for assessing cancer expansion directions. Skeletal type of a developing pattern in 2D, 3D breast images shows the expanding ways is the focal thought for this technique. Breast disease expands in all potential ways dependent on different physiological states of the encompassing regions. Moreover, one can anticipate future directions of expanding the cancer disease on the past directional spread. This may not give exceptionally exact outcomes since future development not just relies upon the present and past status, yet in addition on the physiological states of the encompassing zones, which are represented by both interior just as outside causal reasons. Be that as it may, overall, present, and past status-based forecast would effectively predict future expansion of the disease. Here a nine-way direction based rectangular digital lattice is proposed to identify for expansion cancer by skeletonization of 2D, 3D breast images.

II. D IMAGES: SKELETONIZATION

2D shaping is the opposite procedure for reducing a 2D image. A square, a rhombus and an subjective shapes are presented in Fig. 1. In Fig.1, results after diminishing S. procedure in particular images are displayed.

'Skeletonization' of a picture is basically a diminishing cycle with the exemption that skeletonization holds all corner pixels. Fig. 2 shows a square, a rhombus and a subjective shape and the consequences of skeletonizing them. Given a 2D mammogram, one ought to have the option to skeletonize it to recognize the ways in which the malignancy has just developed or expanding.

A. Process to Skeletonize a 2D digital image by reducing method

Examine a given image pixel wise with 3x3 void window. Follow the procedure at each position. Under the filtering window peruse the picture pixels. Discover the biggest pixel esteem (R,G,B) and the littlest incentive among the threesteems. Now, define the threshold value. Keep the central pixel value as it is, if the difference between lowest and biggest pixel values are lower or equal to the threshold value then remove all boundaries other than corner pixels of the sub image scanned by the window. Move the filtering window to the following position if the difference value is more than the threshold value. Repeat the same procedure so that the image reduced by one limit. Repeat the same procedure so that the image does not show any limits. At last, one shows up at the totally reduced picture with all limits eliminated. The divided and binarized form of Breast cancer disease information is shown in Fig. 3 as an example. Breast Cancer disease and the ways of expanding is shown in Fig. 4

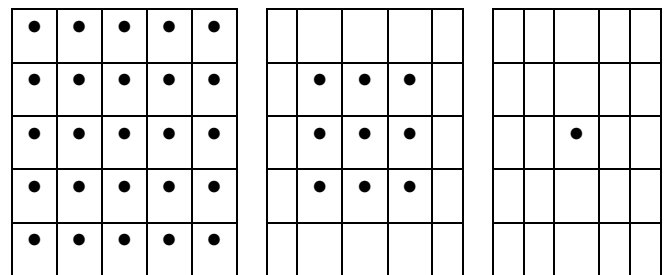


Fig. 1: Thinning process of hypothetical 2D images

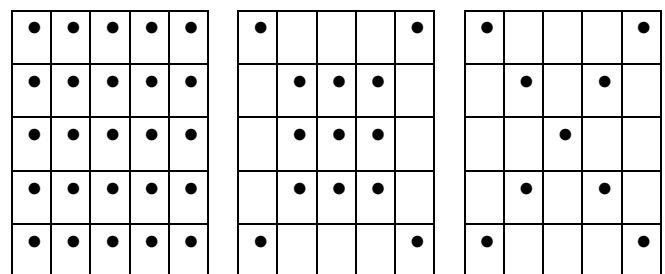
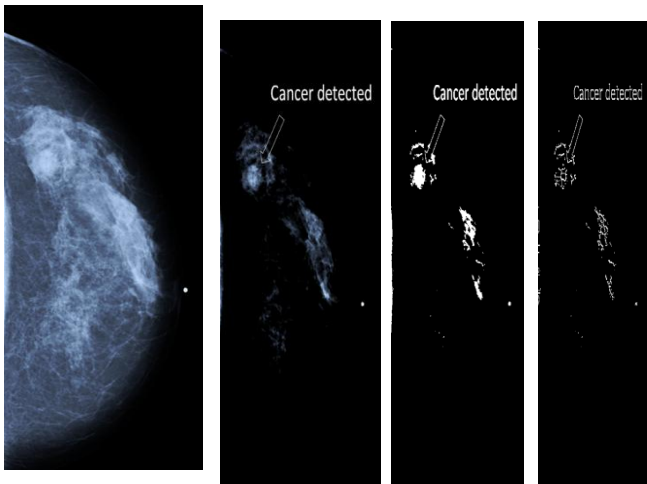


Fig. 2: Skeletonization process of hypothetical 2D images

Revised Manuscript Received on November 20, 2020.

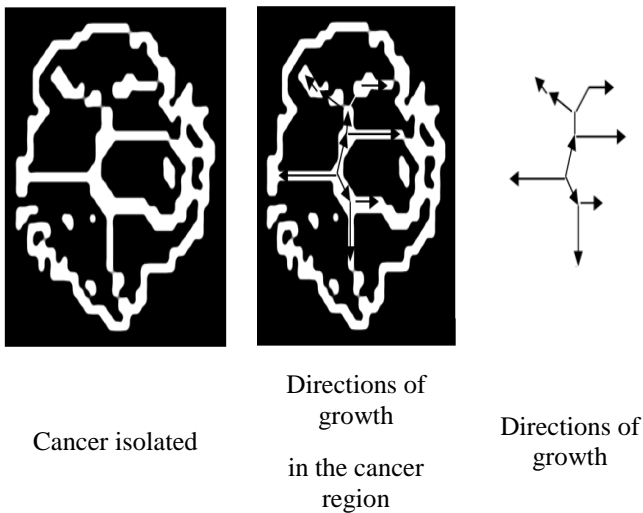
Madhavi Pingili*, Research Scholar, Dept. of Computer Science, MG-NIRSA, Affiliated to University of Mysore, Manasagangotri, Mysore, Karnataka, India. E-mail: madhavipingili@gmail.com

Prof. E.G. Rajan, Director, MG-NIRSA, University of Mysore, Mysore, India. Email: dr.rajaneg@gmail.com



Tomo-synthesized breast cancer image slice, Segmented image, Binarized and cancer isolated image, Skeletonized Version

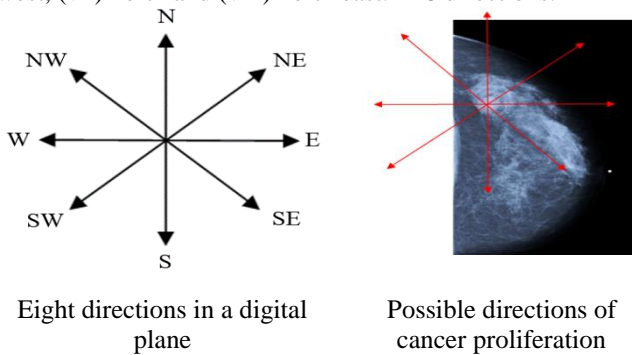
Fig. 3: Sample breast cancer image and its segmented, binarized and skeletonized versions



Directions of growth in the cancer region, Directions of growth

Fig. 4: Skeleton of breast cancer and its proliferation directions

Fig. 5 displays the directions of 2D image namely (i) east, (ii) south east, (iii) south, (iv) south west, (v) west, (vi) north west, (vii) north and (viii) north east. In 8 directions.



Eight directions in a digital plane, Possible directions of cancer proliferation

Fig. 5: Eight directions in a digital plane and directions of cancer proliferation

B. Cancer Expansion: Directions

One can expect cancer proliferation in all possible combinations of eight directions.

$${}^8C_0 = 1, {}^8C_1 = 8, {}^8C_2 = 28, {}^8C_3 = 56, {}^8C_4 = 70, {}^8C_5 = 56, {}^8C_6 = 28, {}^8C_7 = 8, {}^8C_8 = 1$$

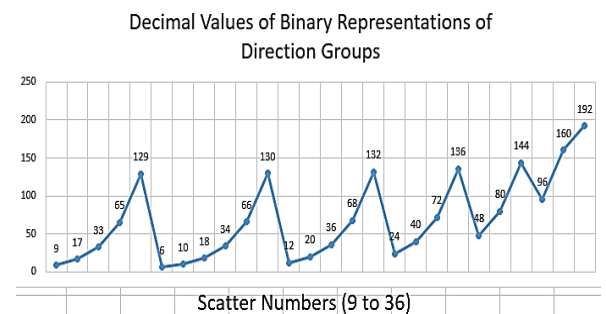
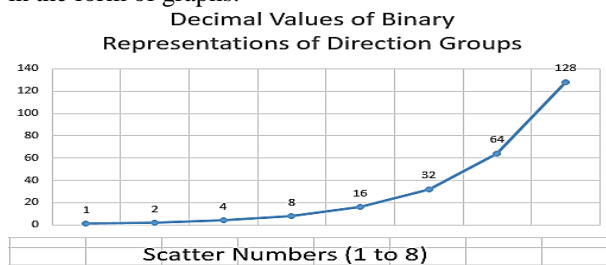
$$\text{Total number of directions in a } 3 \times 3 \text{ rectangular lattice} = \sum_{i=0}^8 {}^8C_i = 256$$

One can attribute quantificational measures to all 256 scatter patterns in the following manner. Presence of a direction is denoted by a '1' and absence by a '0'. Hence, one can have 256 binary patterns of length 8 and the corresponding decimal values. First 20 scatter patterns are given in Table 1. Each pattern has a degree, that is number of links (directions) attached to the central node.

Table I: Binary representations of scatter patterns along with decimal equivalents

Sl. No.	Scatter Number	Degree	North East	North	North West	West	South West	South	South East	East	Decimal Value
1	0	0	0	0	0	0	0	0	0	0	0
2	1	1	0	0	0	0	0	0	0	1	1
3	2	1	0	0	0	0	0	0	1	0	2
4	3	1	0	0	0	0	0	1	0	0	4
5	4	1	0	0	0	0	1	0	0	0	8
6	5	1	0	0	0	1	0	0	0	0	16
7	6	1	0	0	1	0	0	0	0	0	32
8	7	1	0	1	0	0	0	0	0	0	64
9	8	1	1	0	0	0	0	0	0	0	128
10	9	2	0	0	0	0	0	1	1	1	3
11	10	2	0	0	0	0	0	1	0	1	5
12	11	2	0	0	0	0	1	0	0	1	9
13	12	2	0	0	0	1	0	0	0	1	17
14	13	2	0	0	1	0	0	0	0	1	33
15	14	2	0	1	0	0	0	0	0	1	65
16	15	2	1	0	0	0	0	0	0	1	129
17	16	2	0	0	0	0	0	1	1	0	6
18	17	2	0	0	0	0	1	0	1	0	10
19	18	2	0	0	0	1	0	0	1	0	18
20	19	2	0	0	1	0	0	0	1	0	34

The decimal representations of scatter patterns are presented in the form of graphs.



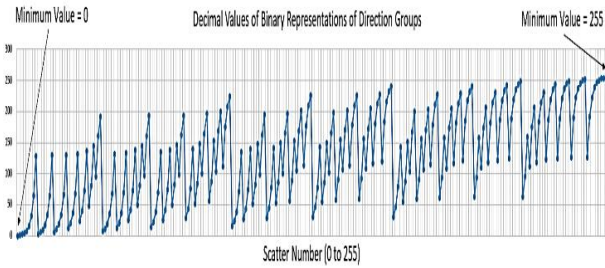


Fig. 6: Graph showing all decimal equivalents of scatter patterns 1 to 254

III. D IMAGES: SKELETONIZATION AND REDUCING

3D image skeletonization process is described in a novel way to explain and estimate in which direction the cancer is moving after getting confirmation from the woman's breast effected by cancer. For instance, onion is taken here as an example for reducing the patterns. Continuously removing the onion skin results the final portion of use. Here onion is a 3D image continuous removing of layers will result final 3D object, which cannot be removed further. Fig. 7 shows the peeling off process of a hypothetical 3D cube like object with a boundary, till a 3D object without boundary is obtained.

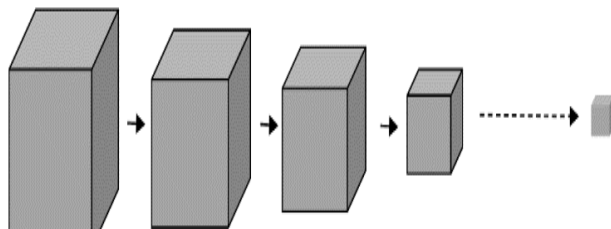


Fig. 7: Thinning process of a cube like solid object

Fig. 8 shows a 3D solid cube of size 100×100×100 and its skeletonized version. It also shows a 3D image called "Cell Fract" and its skeletonized version.

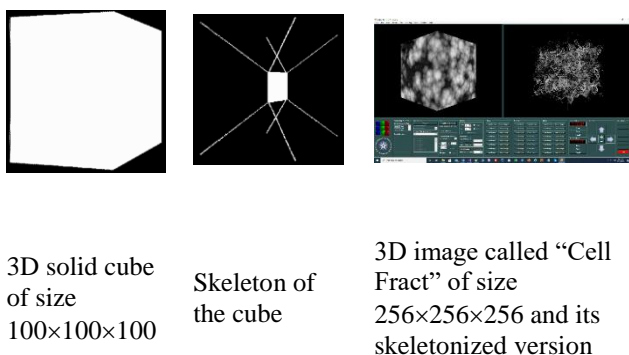


Fig. 8: Skeletonization of 3D images

A. Process to Skeletonize a 3D digital image

Pixel wise Scan the 3D image with 3x3x3 void window. Repeat the below process at each point. Under the 3D scanning window read the pixel of the image. Among 3x3x3 values identify the biggest pixel (RGB). Note the gap between smallest and biggest pixel values. Now, define the threshold value. Keep the central pixel value as it is, if the difference between smallest and biggest pixel values are lower or equal to the threshold value then remove all

boundaries other than corner pixels of the 3D image scanned by the window. Move the filtering window to the following position if the difference value is more than the threshold value. Repeat the same procedure so that the 3D image reduced by one limit. Repeat the same procedure so that the 3D image does not show any limits. At last, one shows up at the totally reduced 3D picture with all limits eliminated except 3D corners.

B. Cancer Expansion directions in a 3D neighborhood of Size 3×3×3

In a 3D advanced picture, one can have 26 bearings from a typical point. So as to have a superior arrangement, let us consider a 3D neighborhood of size 3×3×3 appeared in Fig. 9(a) and Fig.9(b). This 3D neighborhood of size 3×3×3 is likewise imagined as a heap of three layers speaking to front plane, center plane and backplane of the structure appeared in Fig. 9(a) and Fig.9(b).

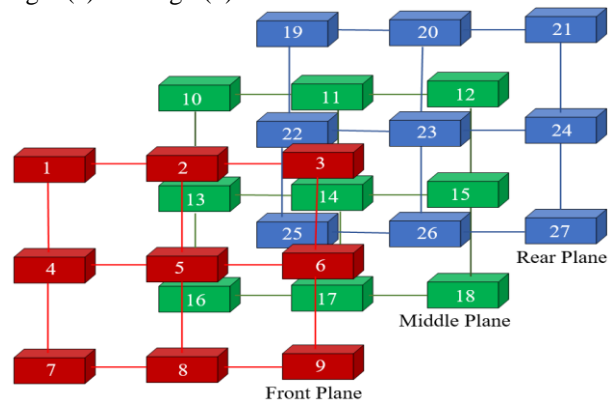


Fig. 9(a): 3D neighborhood structure of size 3×3×3 with labeled vertices

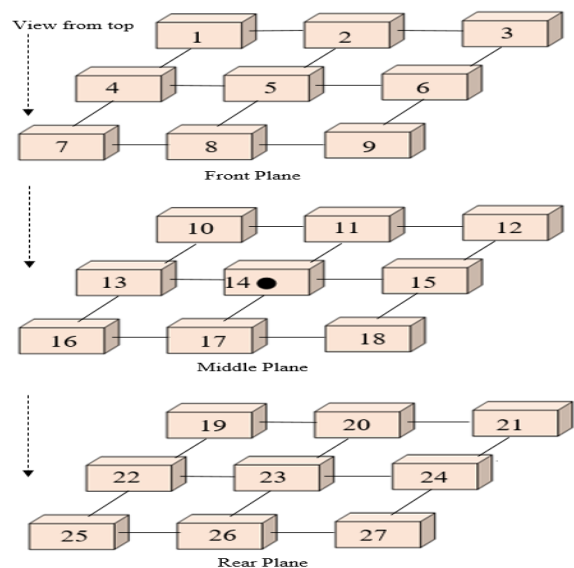


Fig. 9(b): 3D neighborhood structure of size 3×3×3 with labeled vertices

There are 26 headings of expansion from the focal cell (fourteenth cell) where malignancy seed is recognized. They are introduced underneath in Table 2. Table 3 presents all out number of blends of 67,108,864 headings called 3D disperse designs.



Table 2: Directions from the central cell 14 to all other 26 vertices

14 → 1	14 → 2	14 → 3	14 → 4	14 → 5	14 → 6	14 → 7
14 → 8	14 → 9	14 → 10	14 → 11	14 → 12	14 → 13	14 → 15
14 → 16	14 → 17	14 → 18	14 → 19	14 → 20	14 → 21	14 → 22
14 → 23	14 → 24	14 → 25	14 → 26	14 → 27		

Table 3: Total of 67,108,864 three-dimensional scatter patterns

${}^{26}C_0 = 1$	${}^{26}C_8 = 1562275$	${}^{26}C_{16} = 5311735$	${}^{26}C_{24} = 325$
${}^{26}C_1 = 26$	${}^{26}C_9 = 3124550$	${}^{26}C_{17} = 3124550$	${}^{26}C_{25} = 26$
${}^{26}C_2 = 325$	${}^{26}C_{10} = 5311735$	${}^{26}C_{18} = 1562275$	${}^{26}C_{26} = 1$
${}^{26}C_3 = 2600$	${}^{26}C_{11} = 7726160$	${}^{26}C_{19} = 657800$	
${}^{26}C_4 = 14950$	${}^{26}C_{12} = 9657700$	${}^{26}C_{20} = 230230$	
${}^{26}C_5 = 65780$	${}^{26}C_{13} = 10400600$	${}^{26}C_{21} = 65780$	
${}^{26}C_6 = 230230$	${}^{26}C_{14} = 9657700$	${}^{26}C_{22} = 14950$	
${}^{26}C_7 = 657800$	${}^{26}C_{15} = 7726160$	${}^{26}C_{23} = 2600$	

Fig. 10 shows some of the scatter patterns.
 Total number of directions in a 3x3x3 rectangular lattice = $\sum_{i=0}^{26} {}^{26}C_i = 67,108,864$

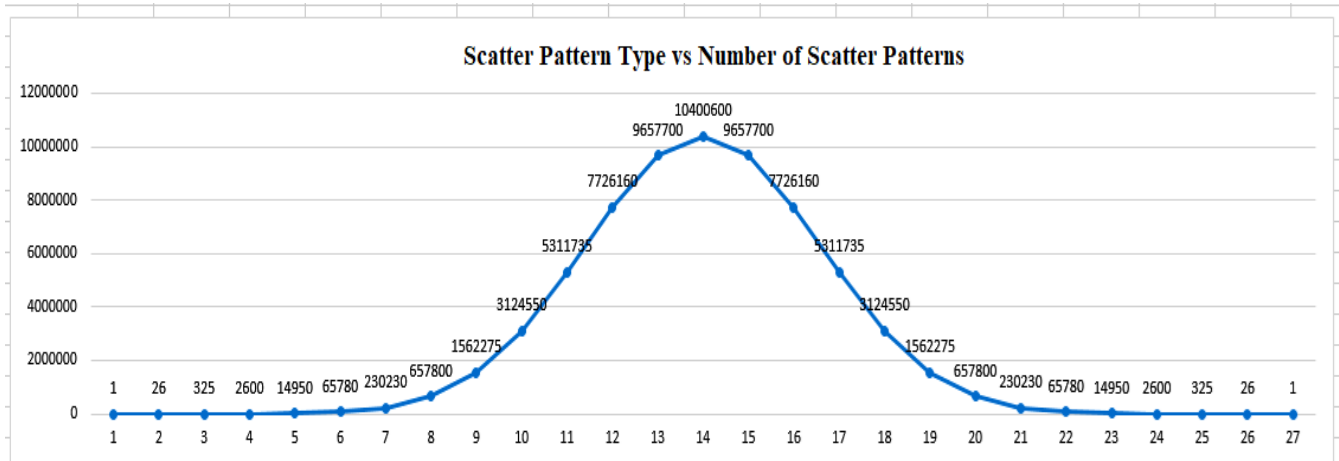


Fig. 10: Scatter pattern types (27) vs number of 3D scatter patterns

IV. RESULTS & OBSERVATIONS

There is only one 3D scatter pattern in this case.

<14→1>, <14→2>, <14→3>, <14→4>, <14→5>, <14→6>, <14→7>, <14→8>, <14→9>, <14→10>, <14→11>, <14→12>, <14→13>, <14→15>, <14→16>, <14→17>, <14→18>, <14→19>, <14→20>, <14→21>, <14→22>, <14→23>, <14→24>, <14→25>, <14→26>, <14→27>



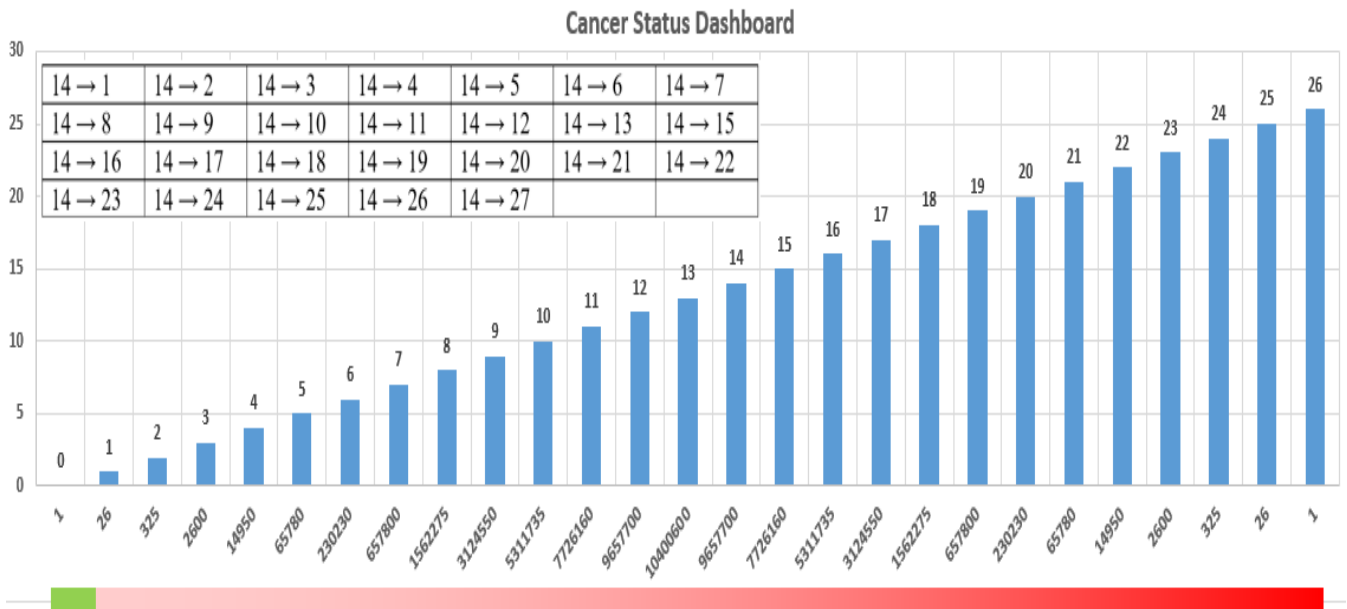


Fig. 11: Cancer status dashboard

V. CONCLUSION

Given a 2D, 3D scanned image of female breast, one can evaluate the present cancer proliferation status using the novel technique introduced in this paper. Skeletonization algorithm is used for this purpose. Unfortunately this technique is not enough to precisely evaluate cancer proliferation since this technique deals with two dimensional images only. Alternatively, if one uses the same technique for evaluating cancer proliferation in a three dimensional image, then the study would be highly fruitful. So Skeletonization algorithm is used for detecting cancer expansion all 4π steradians. With reference to Fig. 9, the degree of a node decides the status of cancer expansion. The node with degree 26 could be seen to show that the cancer status has reached the final stage and this indicates the necessity to go in for surgery such as lumpectomy, quadrantectomy, partial mastectomy, or segmental mastectomy meaning removal only the part of the breast containing the cancer.

REFERENCES

1. A. J. Mendez, P. G. Tahoces, M. J. Lado, M. Souto, and J. J. Vidal, "Computer-aided diagnosis: Automatic detection of malignant masses in digitized mammograms," *Med Phys.*, vol. 25, pp. 957–64, Jun. 1998.
2. J. Tang, R. Rangayyan, J. Xu, I. E. Naqa, and Y. Yang, "Computer aided detection and diagnosis of breast cancer with mammography: Recent advances," *IEEE Trans. Inf. Technol. Biomed.*, vol. 13, no. 2, pp. 236–251, Mar. 2009.
3. M. Ladekarl, "Objective malignancy grading: A review emphasizing unbiased stereology applied to breast tumors," *APMIS Suppl.*, vol. 79, pp. 1–34, 1998.
4. T. M. Haygood, G. J. Whitman, E. N. Atkinson, R. G. Nikolova, S. Y. Sandoval, and P. J. Dempsey, "Results of a survey on digital screening mammography: Prevalence, efficiency, and use of ancillary diagnostic AIDS," *J. Amer. Coll. Radiol.*, vol. 5, pp. 585–92, Apr. 2008.
5. R. Schulz-Wendtlund, K. P. Hermann, T. Wacker, and W. Bautz, "Current situation and future perspectives of digital mammography," *Radiologe*, vol. 48, pp. 324–34, Apr. 2008.

AUTHORS PROFILE



P. Madhavi, completed her B.Tech-CSIT, M.Tech-IT and pursuing Ph.D-CS from University of Mysore. Her area of interest is in Image Processing, AI, Data Mining, Machine Learning.



Dr. E G Rajan, done his Ph.D form IIT-Kanpur. His area of interest is in Signal and Image Processing, Data Mining, Machine Learning.

